

SUPPLEMENTAL MATERIAL

Hippo-Yap signaling maintains sinoatrial node homeostasis

Running title: Hippo signaling maintains sinoatrial node homeostasis

Mingjie Zheng, PhD; Rich Gang Li, PhD; Jia Song, MD; Xiaolei Zhao, PhD; Li Tang, MS; Shannon Erhardt, MS; Wen Chen, BS; Bao H. Nguyen, BS; Xiao Li, PhD; Min Li, PhD; Jianxin Wang, PhD; Sylvia M. Evans, PhD; Vincent M. Christoffels, PhD; Na Li, PhD; Jun Wang, PhD

Correspondence

Jun Wang, PhD, Department of Pediatrics, McGovern Medical School, Graduate School of Biomedical Sciences, The University of Texas Health Science Center at Houston, Texas 77030, USA.

E-mail: jun.wang@uth.tmc.edu

Department of Pediatrics, McGovern Medical School, The University of Texas Health Science Center at Houston (M.Z., X.Z., S.E., W.C., J.W.), MD Anderson Cancer Center and UTHealth Graduate School of Biomedical Sciences, The University of Texas, Houston, Texas, USA (S.E., J.W.). Texas Heart Institute, Houston, Texas, USA (R.G.L., X.L.). Department of Molecular Physiology and Biophysics (B.H.N.), Department of Medicine (Section of Cardiovascular Research), Cardiovascular Research Institute, Baylor College of Medicine, Houston, TX, USA (J.S., N.L.). Hunan Provincial Key Lab on Bioinformatics, School of Computer Science and Engineering, Central South University, Changsha, Hunan, China (L.T., M.L., J.W.). Skaggs School of Pharmacy and Pharmaceutical Sciences, Departments of Pharmacology and Medicine, University of California at San Diego, La Jolla, CA 92093, USA (S.M.E.). Medical Biology, Amsterdam Cardiovascular Sciences, Amsterdam UMC, University of Amsterdam, Amsterdam, The Netherlands (V.M.C.).

Supplemental Methods

Telemetry Electrocardiogram (ECG)

Implantation of the intraperitoneal telemetry transmitters ETA-F10 (Data Sciences International, St Paul, MN) was done by following the protocol provided by the manufacturer. ECG leads were placed in the lead II configuration. 24 hours ECG data was collected using DSI Telemetric Physiological Monitor System and processed by Ponemah Physiology Platform software (Data Science International, St Paul, MN). Signal average and Poincaré plots were generated with a custom MATLAB script.

5-ethynyl-2'-deoxyuridine (EdU) staining, Masson's trichrome staining, immunohistochemistry, and fluorescence in situ hybridization

Before the heart was harvested, EdU (0.5 mg) was intraperitoneally injected into mice for 4 consecutive days. After EdU injection, the heart was collected at 8 days after tamoxifen injection. Hearts were embedded in paraffin using standard protocol and sectioned at a thickness of 7 μ m. EdU staining was assayed using the Click-iT EdU Alexa Fluor 647 imaging kit (Life Technologies C10340). SB431542 (TGF- β 1 receptor inhibitor, selleckchem, S1067) was intraperitoneally injected into mice at 10 mg/kg for 5 consecutive days, performed two days before EdU injection. Masson's Trichrome staining was performed according to manufacturer's instruction (Sigma, HT15). Images were captured on a LAS X imaging system (Leica). Immunohistochemistry (IHC) was performed followed standard protocol. Antibodies used in this study were as follows: rat anti-Hcn4 (1:100 dilution; Abcam, ab32675), rabbit anti-pYap (1:100 dilution; Cell signaling technologies 4911), rabbit anti-active Yap (1:100 dilution; Abcam, ab205270), rabbit anti-Collagen 1 (1:100 dilution; Abcam, ab21286), rabbit anti-Vimentin (1:100 dilution; Abcam, ab92547), mouse anti-cTnT (1:200 dilution; Thermo, MA5-12960), mouse anti-Ryanodine Receptor (1:100 dilution; Abcam, ab2868), and mouse anti-pSmad3 (1:100 dilution; Santa Cruz Biotechnology, sc-517575). Fluorescence in situ hybridization using Probe-Mm-*Tgfb1* (ACD, 407751) using RNAscope followed manufacturer's instructions in the RNAscope 2.5 HD Assay-RED protocol (ACD). Nuclei were stained with 4,6-diamidino-2-phenylindole (DAPI). Wheat germ agglutinin (WGA) conjugates were added to outline cell membrane. Fluorescence images were captured on a Zeiss confocal microscope with ZEISS ZEN microscope software.

Quantitative real-time PCR (qRT-PCR)

The hearts were removed quickly from mice and placed in the Tyrode's solution containing: 1.2 mM KH_2PO_4 , 140 mM NaCl, 5 mM HEPES, 5.4 mM KCl, 5.55 mM glucose, 1.0 mM MgCl_2 , and 1.8mM CaCl_2 (pH was adjusted to 7.4 with NaOH). The SANs were dissected from the region bordered by the crista terminalis, interatrial septum, the inferior and superior vena cavae. Total RNA of adult mouse SAN tissues was extracted using the RNeasy Micro Kit (Qiagen). Purified RNA was reverse-transcribed by the iScript Reverse Transcription Supermix (Bio-Rad, Hercules, CA, USA). The SYBR Green PCR Master Mix (Applied Biosystems, Waltham, MA, USA) was used for real-time thermal cycling (Applied Biosystems, Waltham, MA, USA).

Confocal Ca^{2+} imaging of pacemaker cells

To record cellular Ca^{2+} , isolated pacemaker cells from SAN tissues were incubated with Fluo-4-AM (2 $\mu\text{mol/L}$, Life Technologies) at room temperature for 30 minutes in Kraft-Brühe (KB) solution, followed by perfusion in normal Tyrode solution. Cells were placed in a chamber and imaged through a 40X oil immersion objective on a confocal microscope (LSM 510, Carl Zeiss AG, Oberkochen, Germany). Fluo-4 was excited at 488 nm with emission collected through a 515 nm long pass filter while fluorescence images were recorded in line-scan mode with 1024 pixels per line at 500 Hz. SR Ca^{2+} content was assessed by rapid application of 10 mM caffeine towards the end of the recording. The fluorescence intensity (F) proportional was analyzed after background subtraction and normalized to baseline fluorescence, F_0 (F/F_0).

Cleavage under targets and tagmentation (CUT&Tag)

Nuclei from SAN tissues were incubated with concanavalin A (Con A)-coated magnetic beads (Bangs Laboratories, BP531) at room temperature for 10 min to immobilize nuclei on the Con A-coated magnetic beads. The bead-bound nuclei were then incubated with anti-H3K4me3 (Active Motif, 39159, 1:100) and anti-Yap1 (Novus, NB110-58358, 1:50) antibodies separately overnight at 4 °C with rotation. Guinea pig anti-rabbit second antibody (Antibodies-Online, ABIN101961, 1:100) was diluted in 50 mL of wash buffer and added into the nucleus to incubate for 30 min at room temperature. The pA-Tn5 adapter complex was diluted 1:200 in 300-buffer and incubated with nucleus at room temperature for 1 h. Nuclei were then resuspended in tagmentation buffer at 37 °C for 1 h for DNA fragmentation. After 1 h, 0.5M EDTA, 10%SDS, and 20mg/mL Proteinase K were added to terminate tagmentation and incubated for 10 min at 70°C. DNA was then purified using

phenol-chloroform-isoamyl alcohol extraction and ethanol precipitation and dissolved in 21 μ L 1 mM Tris-HCl at pH 8 and 0.1 mM EDTA. The libraries were prepared by adding 2 μ L of 10 μ M barcoded i5 primer, 2 μ L of 10 μ M uniquely barcoded i7 primers, and 25 μ L NEBNext HiFi 2X PCR Master mix (Biolabs, M0541L), and PCR was performed according to the conditions in the protocol. AMPure XP beads (Beckman Coulter, A63880) were used for DNA purification. Libraries were sequenced on NextSeq 550 (Illumina, USA) at UTHealth Cancer Genomics Center, and 75-bp paired-end reads were generated. Fastp software was used to remove adaptor and low-quality reads. All reads produced by CUT&Tag of H3K4me3 were aligned to the hg19 human genome using BWA (Burrows-Wheeler Aligner). MACS2 was used for peak calling. Genes with a peak within 3 kb of the transcription start site (TSS) were considered target genes. An area of 6 kb surrounding each TSS was selected to get CUT&Tag profiles of H3K4ac using deepTools software. Annotation of peaks was performed using ChIPseeker. The CUT&Tag sequencing datasets have been deposited to the National Center for Biotechnology Information Gene Expression Omnibus under the accession number of GSE202641.

Cut&Tag data processing

The paired-end FASTQ format raw reads were aligned to mm10 by Bowtie2 using parameters “--end-to-end --very-sensitive --no-mixed --no-discordant --phred33 -I 10 -X 700”, then the duplicates were removed by Picard, and the low-quality mapped reads were filtered by Samtools with the minimum quality score of 30. To construct the UCSC visualization tracks, we converted alignment files into bigwig and bedgraph format with bamCoverage of deepTools. Then SEACR was used to call peaks with “stringent” and “norm” mode, the IgG alignment file was used as the control data. The called peaks were annotated by the annotatePeaks function of Homer, then the read heatmaps of called peaks were generated with plotHeatmap of deepTools. The top enriched motifs were detected by the findMotifsGenome function of Homer with size of 200. In addition, Gene Ontology (GO) analysis was performed by processing processed dataset using Metascape, which provided multiple defined terms that represented gene properties containing cellular component, molecular function and biological process. Yap1 and H3K4me3 peaks were called using IgG signals as background, using the SEACR-norm option. Total of 67,341, 39,920 and 55,494 peaks were called from control Yap1, LatsCKO Yap1, and H3K4me3 samples, respectively. Subsequent known motif enrichment analysis was performed using Homer version 4.11, using findMotifsGenome.pl function with

parameters: -size 200 -mask. Heatmaps of CUT&Tag signals on peaks were visualized by deepTools and genomic tracks were visualized by UCSC genome browser. Density of H3K4me3 signals on Yap1 binding sites were quantified by calculating the mean levels of normalized density within the peak center ± 200 bp region for each peak.

ATAC-seq data processing and analysis

Raw ATAC-seq reads of PC and RACM ATAC-seq data (GSE148515) were mapped to the mm10 build of the mouse genome using BWA with default settings. SAMtools was used to merge the replicate BAM files. Bigwig file was generated using the bamCoverage function of deepTools (3.5.1). Then, the bigwig file was uploaded to the UCSC genome browser for visualization.

For SANLPC and VLCM ATAC-seq data (GSE146044), raw ATAC-seq reads for GSE146044 were mapped to the hg19 build of the mouse genome using BWA with default settings. SAMtools was used to merge the replicate BAM files. Bigwig file was generated using the bamCoverage function of deepTools (3.5.1). The bigwig file was converted to the reference of mm10 by CrossMap (0.6.1). Then, the lift-over bigwig file was uploaded to the UCSC genome browser for visualization.

Conserved sequence analysis

The phastCons60way score file of mm10 was downloaded from UCSC. The phastCons60 used to calculate the conservation score was based on 60 vertebrate species including humans. The Yap binding peaks located at *Ryr2*, *Tgfb1*, and *Tgfb3* were extracted from Yap Cut&Tag seq data and extended to 200 bp respectively, which were prepared as bed format files. We employed “ComputeMatrix” function in deepTools to calculate the signal distribution relative to the center of peaks, the non-overlapping bins for averaging the score were set to 10, and the distance upstream/downstream of the peak center was set 500bp, the regions with only scores of zero were skipped. Then the calculated signal matrix was imported to “plotProfile” function to generate the conservation score plot.

Western Blotting (WB)

SAN tissues were dissected from adult mice hearts and snap-frozen in liquid nitrogen. SANs from 7 mice for control and *Lats1/2* CKO groups were pooled and stored at -80 °C. For protein extraction, samples were homogenized in RIPA buffer (25mM Tris-HCl (pH 7.6), 150mM NaCl, 1% NP-40, 1% sodium deoxycholate, 0.1% SDS) with protease and

phosphatase inhibitor cocktail tablets (Roche, West Sussex, UK) at 4 °C. Extracts were then centrifuged at 13,000×g for 10 min at 4 °C. For Western blot analysis, the proteins were loaded and separated by SDS-PAGE and transferred onto a polyvinylidene difluoride membrane (Millipore, IPVH00010). The membranes were blocked in 5% milk/tris-buffered saline with Tween-20 for 1 h at room temperature and incubated with primary antibodies overnight at 4 °C. The membranes were incubated with secondary horseradish peroxidase (HRP)-conjugated antibodies for 2 h at room temperature and were imaged by Bio-rad imaging systems. Protein bands were visualized using enhanced chemiluminescence (ECL) reagents (Bio-Rad, 170-5061). The following antibodies were used: anti-GAPDH (Abcam, ab9485, 1:2000); anti-pSmad3 (Santa Cruz Biotechnology, sc-517575 1:1000); anti-Ryanodine Receptor (Invitrogen, MA3-916, 1:1000).

Quantification and Statistical analysis

Fiji software was used for intensity analysis of immunofluorescence signal, cell size measurement and cell counting. For 2 groups, statistical significance was determined by t tests if the data was conforming to normal distribution; statistical significance was determined by the Mann-Whitney test if the data was not normally distributed. Statistical significance was determined by one-way ANOVA with post hoc Tukey's tests if the data from more than 2 groups was conforming to normal distribution; Kruskal-Wallis tests with post hoc Dunn's tests were used for not normally distributed data from more than 2 groups. All tests were two-tailed, and all assumptions of normality were assessed using the Shapiro-Wilks test. All statistical analyses and bar graphs were performed using GraphPad Prism version 7.0.

Supplemental Figures and Figure Legends

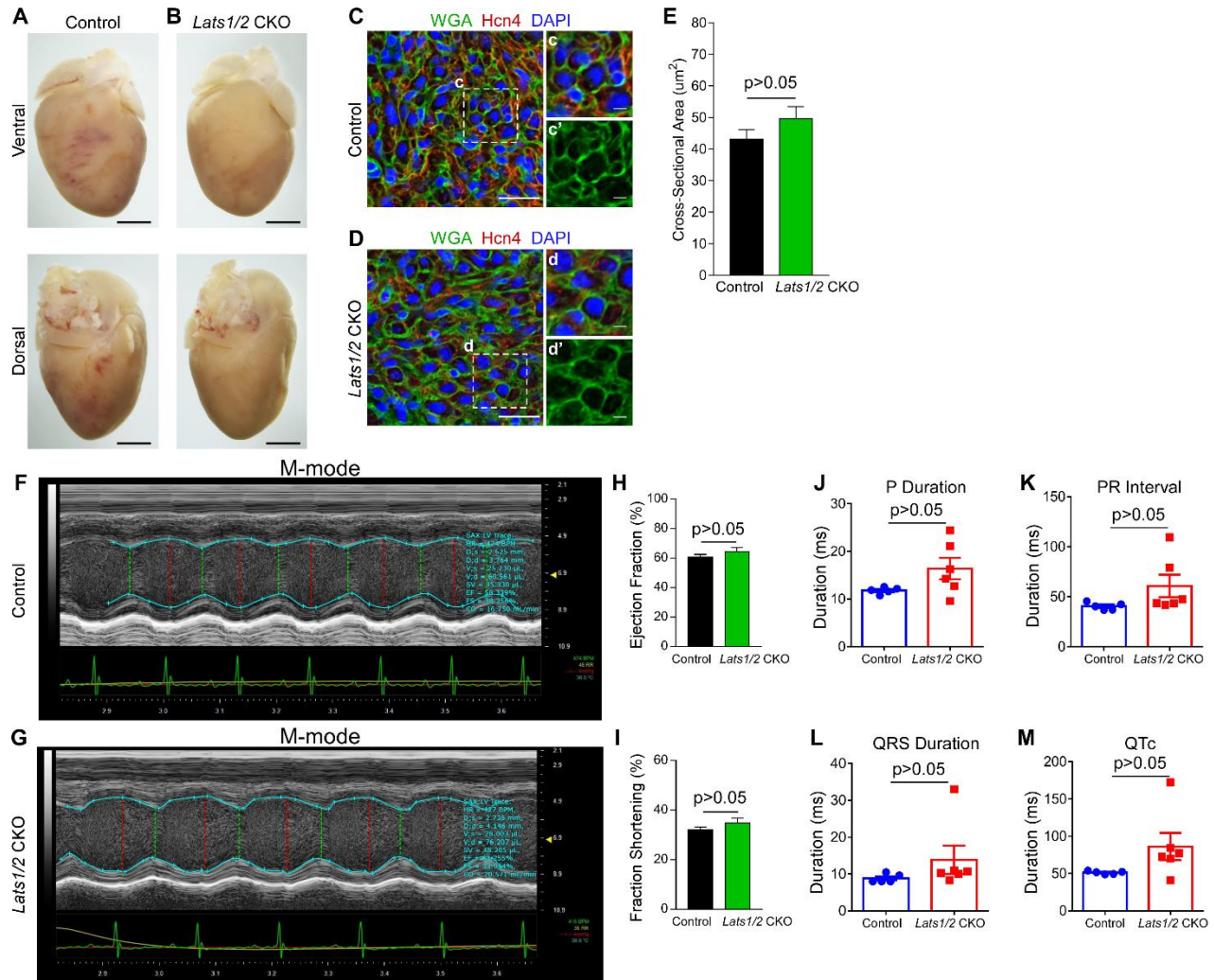


Figure S1. *Lats1* and *Lats2* deletion in the CCS does not cause cardiac structure and function change.

A-B. Representative gross heart morphology at 8 days after Cre activation. Scale bar, 200 μm .

C-E. Wheat germ agglutinin (WGA) staining in control (**C**) and *Lats1/2* CKO (**D**) SANs. Cross-sectional area was measured in the transverse plane. Pacemaker cell size of sinoatrial node has no significant change in mutants compared with controls (**E**). Data are shown as means \pm s.e.m. Statistical significance was determined by Mann–Whitney test, $p > 0.05$. Scale bar, 25 μm , 5 μm .

F-I. Representative M-mode echocardiogram traces of control and *Lats1/2* CKO mouse hearts 8 days after tamoxifen induction. Percent ejection fraction (EF) (**H**), and fractional shortening (FS) (**I**) as determined by echocardiography. Data are shown as means \pm s.e.m; statistical significance was determined by t-test, $p > 0.05$.

J-M. P duration (**J**), PR interval (**K**), QRS duration (**L**) and QTc (**M**) from control ($n=5$) and

Lats1/2 CKO (n=6) mice. Data (H-K) are shown as means \pm s.e.m. Statistical significance was determined by t-test, $p > 0.05$.

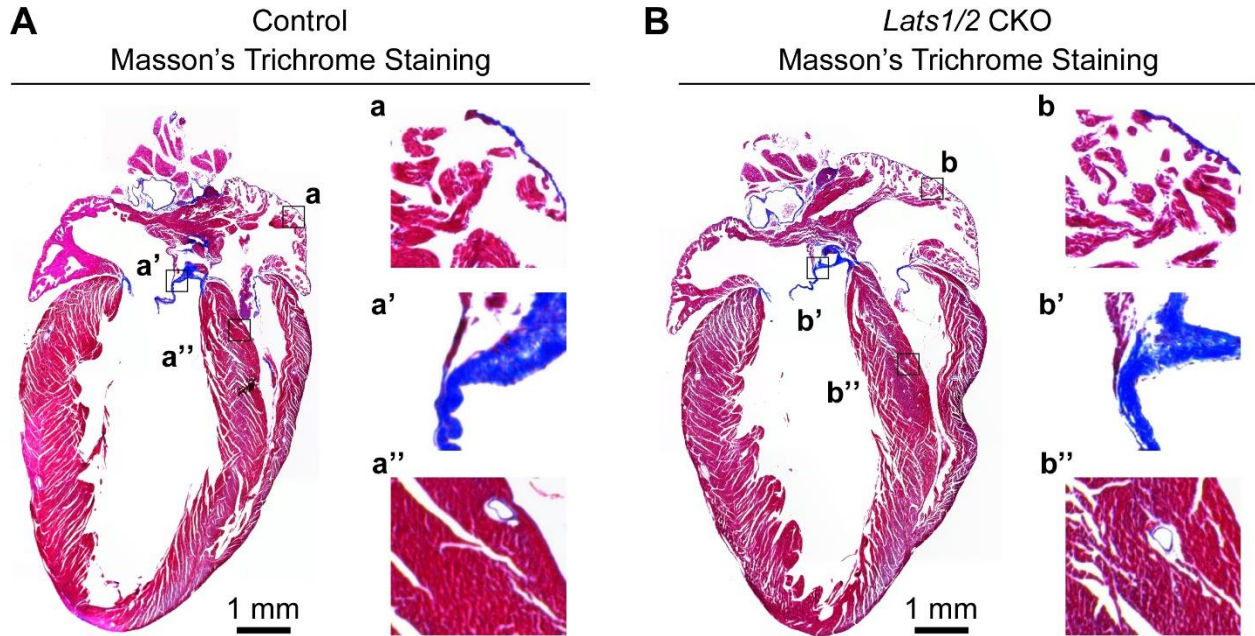
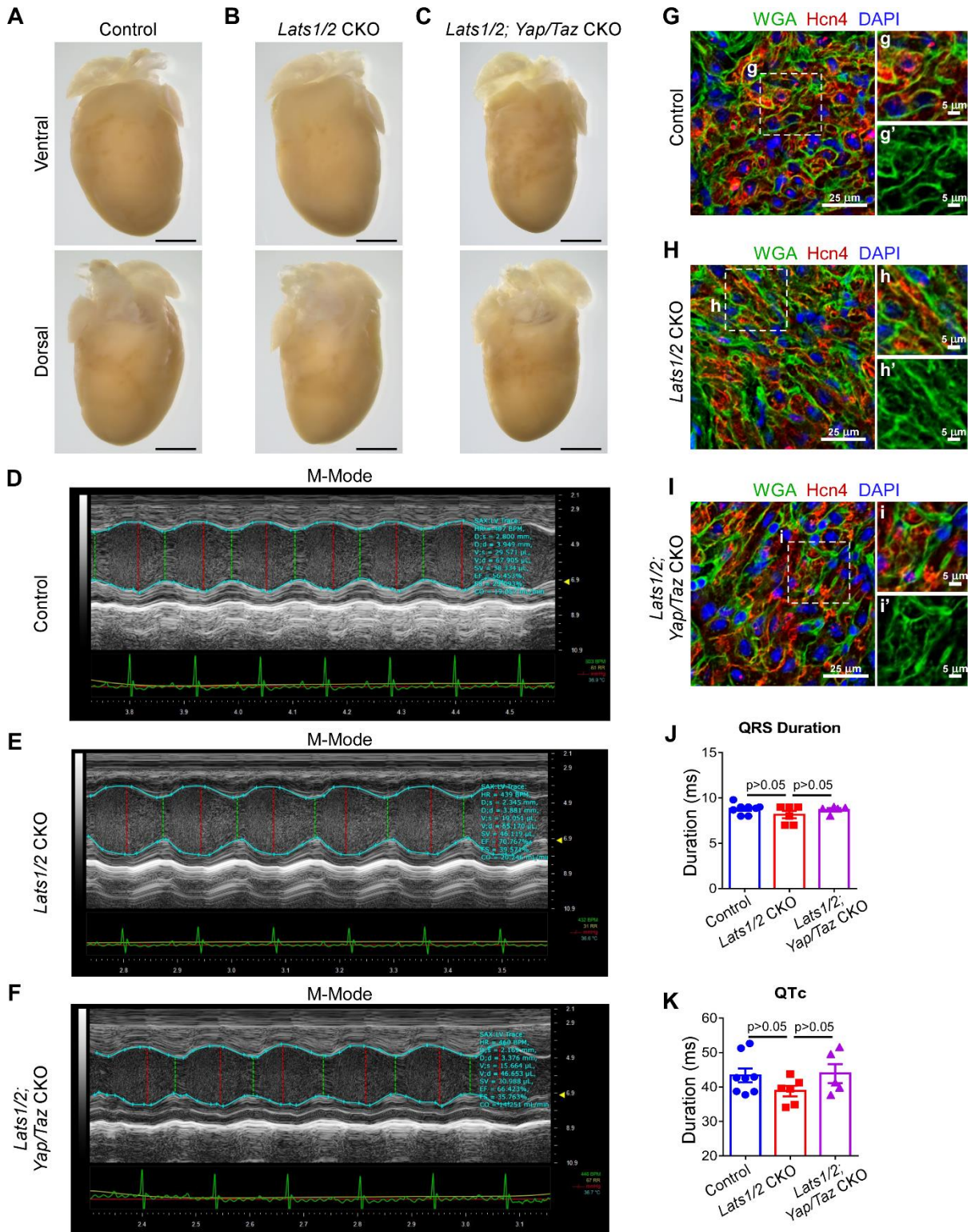


Figure S2. *Lats1* and *Lats2* deletion in the CCS does not cause obvious fibrosis changes in other cardiac structures.

A-B. Masson's Trichrome staining in control and *Lats1/2* CKO hearts. Compared with controls (**A**), *Lats1/2* CKO mice (**B**) did not show histological and fibrotic change in the atria (a and b), valves (a' and b'), or interventricular septum (a'' and b''). Scale bar, 1 mm.



μm . **D-F**. Representative M-mode echocardiogram traces of control, *Lats1/2* CKO, and *Lats1/2; Yap/Taz* CKO mouse hearts 8 days after tamoxifen induction. **G-I**. Wheat germ agglutinin (WGA) staining in control (**G**), *Lats1/2* CKO (**H**), and *Lats1/2; Yap/Taz* CKO (**I**) SANs. Scale bar, 25 μm , 5 μm . **J-K**. QRS duration (**J**) and QTc (**K**) from control (n=8), *Lats1/2* CKO (n=7), and *Lats1/2; Yap/Taz* CKO (n=5) mice. **J** and **K** Data are shown as means \pm s.e.m. Statistical significance was determined by one-way ANOVA, $p > 0.05$.

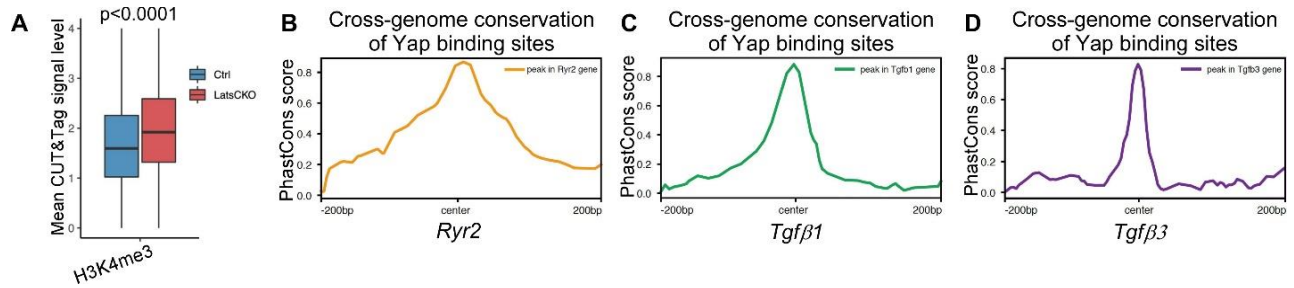


Figure S4. Yap binding sites are enriched by *Lats1/2* deletion and are evolutionarily conserved among vertebrate species.

A. As indicated by H3K4me3 signals, Yap binding activities were significantly increased in *Lats1/2* CKO SANs compared with control SANs. **B-D.** Yap binding sites are overall conserved among vertebrate species. Conservation scores were based on 60 vertebrate species including humans. Representative figures showing the cross-genome conservation scores of Yap binding regions in *Ryr2* (**B**), *Tgfb1* (**C**), and *Tgfb3* (**D**).

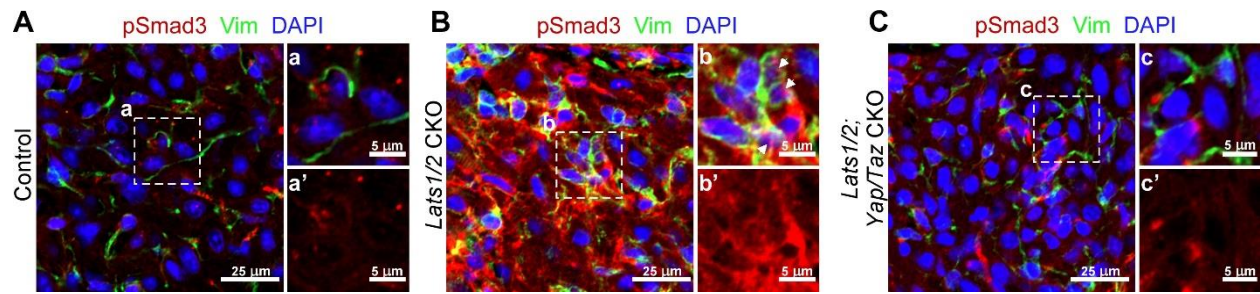


Figure S5. Rescued TGF- β signaling activity in *Lats1/2*; *Yap/Taz* CKO SANs.

A-C. Representative immunofluorescence confocal images of pSmad3 from control (**A**), *Lats1/2* CKO (**B**) and *Lats1/2*; *Yap/Taz* CKO (**C**) SANs. Vimentin (Vim) stained with green and nuclei stained with blue. Panels on the right show higher magnification of the boxed area in panels on the left. Arrows, pSmad staining in nuclei. Scale bar, 25 μ m and 5 μ m.

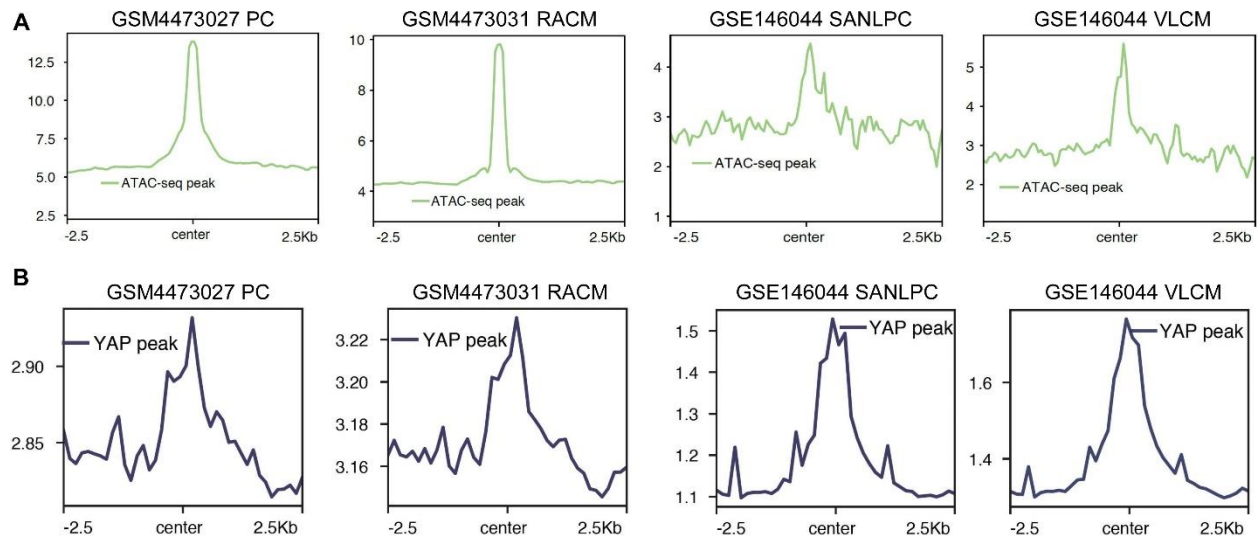


Figure S6. Aligned analysis of ATAC-seq data and CUT&Tag seq YAP peaks.

Yap binding peaks in CUT&Tag seq were mapped to ATAC-seq at genome wide, then mapped ATAC-seq reads were normalized by the effective genome size, and normalized values were regarded as signal scores. Signal scores were used to generate the signal plot. **A.** The signal profile of ATAC-seq peaks for PC, RACM, SANLPC and VLCM ATAC-seq datasets, respectively. **B.** The signal profile of Yap binding peaks for PC, RACM, SANLPC and VLCM ATAC-seq datasets, respectively. PCs, pacemaker cells; RACM, right atrial cardiomyocytes; SANLPC, SAN-like pacemaker cells; VLCM, ventricle-like cardiomyocyte.

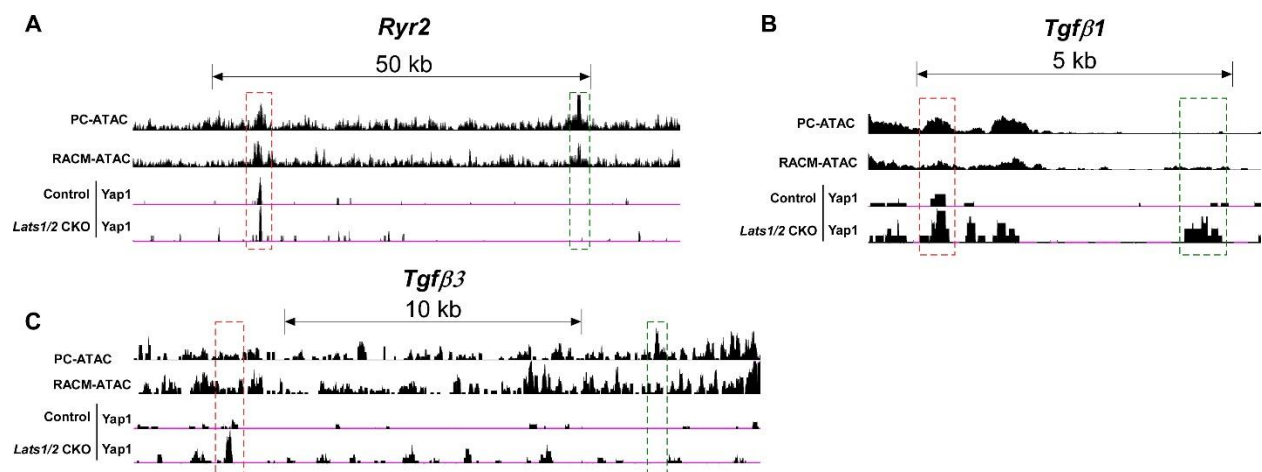


Figure S7. Comparative analysis of neonatal mouse PC and RACM ATAC-seq data and adult mouse SAN CUT&Tag data.

A. Comparative analysis of Yap binding regions and chromatin accessibility in *Ryr2*. **B.** Comparative analysis of Yap binding regions and chromatin accessibility in *Tgfβ1*. **C.** Comparative analysis of Yap binding regions and chromatin accessibility in *Tgfβ3*. PCs, pacemaker cells; RACM, right atrial cardiomyocytes. Red boxed regions show peaks that are consistent among datasets, and green boxed regions show peaks that are different among datasets.

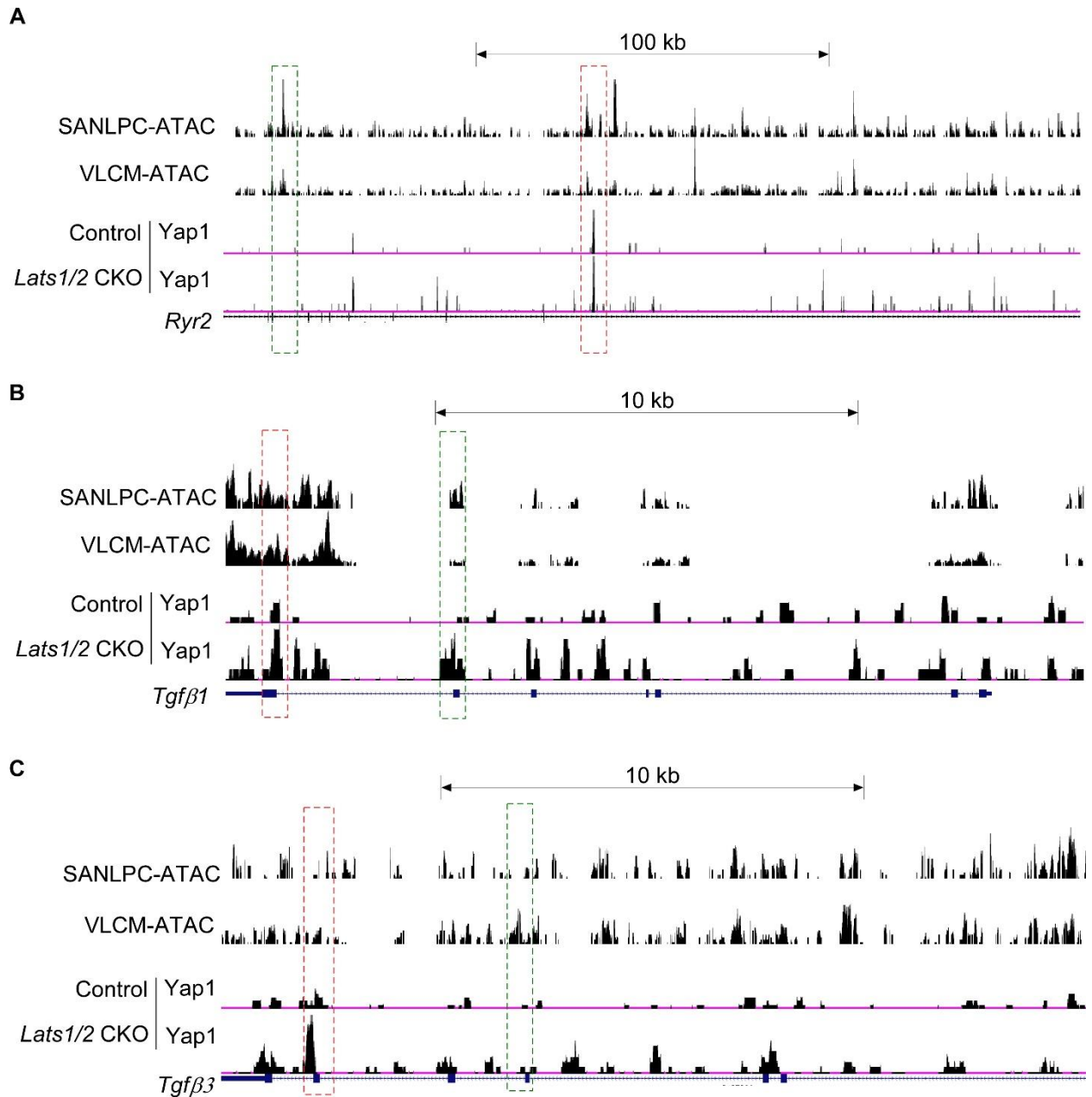


Figure S8. Comparative analysis of human SANLPC and VLCM ATAC-seq data and mouse SAN CUT&Tag data.

A. Comparative analysis of YAP binding regions and chromatin accessibility in *Ryr2*. **B.** Comparative analysis of YAP binding regions and chromatin accessibility in *Tgfb1*. **C.** Comparative analysis of YAP binding regions and chromatin accessibility in *Tgfb3*. SANLPC, SAN-like pacemaker cells; VLCM, ventricle-like cardiomyocyte. Red boxed regions show peaks that are consistent among datasets, and green boxed regions show peaks that are different among datasets.

Supplemental Table**Table S1. Echocardiographic measurement parameters in control and *Lats1/2* CKO mice**

	Control (n=8)	<i>Lats1/2</i> CKO (n=7)
LVID;d (mm)	3.71 ±0.17	3.72 ±0.08
LVID;s (mm)	2.90 ±0.11	2.62 ±0.09
LVPW;d (mm)	0.94 ±0.09	1.07 ±0.16
LVPW;s (mm)	1.11 ±0.12	1.25 ±0.10
LV Vol;s (uL)	26.74 ±1.46	22.93 ±1.99
LV Vol;d (uL)	68.12 ±1.95	64.85 ±3.61
SV (ul)	41.38 ±1.39	41.92 ±2.92
CO (mL/min)	18.85 ±0.78	15.59 ±1.36
EF (%)	60.83 ±1.61	64.56 ±2.59
FS (%)	32.16 ±1.12	34.92 ±1.96

Echocardiographic measurements are from M-mode images. All values expressed are mean ± SEM. d, in diastole; s, in systole; LVID, left ventricle internal diameter; LVPW, left ventricle posterior wall; LV Vol, left ventricle volume; SV, stroke volume; CO, cardiac output; EF, ejection fraction; FS, fractional shortening. No significant difference was observed between groups.